Siberian Branch of Russian Academy of Science
BUDKER INSTITUTE OF NUCLEAR PHYSICS

V.S. Fadin, D.Yu. Ivanov and M.I. Kotsky

ON THE CALCULATION OF THE NLO VIRTUAL PHOTON IMPACT FACTOR

Budker INP 2002-60

Novosibirsk
2002

On the calculation of the NLO virtual photon impact factor[1]

V.S. Fadin[a,b] †, *D.Yu. Ivanov*[c,e] ‡ *and M.I. Kotsky*[a] ††

[a] Budker Institute for Nuclear Physics, 630090 Novosibirsk, Russia

[b] Novosibirsk State University, 630090 Novosibirsk, Russia

[c] Institute of Mathematics, 630090 Novosibirsk, Russia

[e] Regensburg University, Germany

Abstract

The virtual photon impact factor is related to the integral from the discontinuity of the photon-Reggeon scattering amplitude on the right cut. It permits to use analytical properties of the scattering amplitude for the calculation of the impact factor in the next-to-leading order and gives a possibility for considerable simplification of the calculation. A part of the diagrams contributing to the impact factor can be treated without their real calculation.

† *e-mail address:* FADIN@INP.NSK.SU

‡ *e-mail address:* D-IVANOV@MATH.NSC.RU

†† *e-mail address:* KOTSKY@INP.NSK.SU

[1] *Work supported in part by INTAS and in part by the Russian Fund of Basic Researches.*

1 Introduction

There are at least two reasons why the total cross section of interaction of photons with large virtualities $\sim Q^2 \gg \Lambda^2_{QCD}$ at high c.m.s. energies $\sqrt{s}$ is an attractive object for theoretical investigation. The first one is that it was experimentally measured (see [1]-[3] and references therein); the second – at large enough Q^2 this cross section can be calculated in the framework of perturbative QCD. The most interesting is the region of so small values of $x = Q^2/s$ where, firstly, the main contribution to the cross section is given by nondecreasing with energy terms, and secondly, resummation of terms of higher orders of perturbation theory enhanced by powers of $\log(1/x)$ is necessary.

The most common basis for such resummation is given by the BFKL approach [4]. This approach in the leading logarithmic approximation (LLA), when only leading terms $(\alpha_s \ln s)^n$ are resummed, was extensively used for theoretical analysis of $\gamma^*\gamma^*$ interaction [5]. Unfortunately, in the LLA neither scale of energy, nor argument of the running coupling constant α_s are fixed, so that for accurate theoretical prediction we have to know the radiative corrections to the LLA. Recently, the radiative corrections to the kernel of the BFKL equation had been calculated [6] - [11] and the kernel for the forward scattering is presently known in the next-to-leading order (NLO) [12, 13]. Attempts to apply it for comparison with the experimental data [14] are encouraging, but for a consistent comparison one needs to know impact factors of colliding particles with the same accuracy as the kernel of the BFKL equation, since in the BFKL approach the cross section of interaction of particles A and B is given by the convolution of the Green's function G for the two interacting Reggeized gluons, which is determined by the kernel of the BFKL equation, with the impact factors Φ_A and Φ_B, which describe the interaction of the colliding particles with the Reggeized gluons:

$$\sigma_{AB}(s) = \int_{\delta-i\infty}^{\delta+i\infty} \frac{d\omega}{2\pi i} \int \frac{d^2q_A}{2\pi \vec{q}_A^{\,2}} \int \frac{d^2q_B}{2\pi \vec{q}_B^{\,2}} \left(\frac{s}{s_0}\right)^{\omega} \Phi_A(\vec{q}_A, s_0)$$
$$\times G_\omega(\vec{q}_A, -\vec{q}_B)\Phi_B(\vec{q}_B, s_0). \qquad (1.1)$$

Here the vector sign is used for vector components transverse to the plane of the initial momenta p_A, p_B, G_ω is the Mellin transform of the Green's function, and s_0 is an appropriately chosen energy scale. The representation (1.1) is valid both in the LLA and in the NLA. In both cases $G_\omega(\vec{q}_A, -\vec{q}_B)$ is scale-independent; the impact factors become scale-dependent in the NLA, in such a way that under variations of s_0 the cross section remains, within the NLA accuracy, unchanged. It was shown in [15] that to the NLA accuracy one can change the scale s_0 in (1.1) for any factorizable scale $f_A f_B$, with f_i depending on $\vec{q}_i$, without changing the Green function, provided that the impact factors are also changed correspondingly.

At the moment NLO impact factors are known for only coloured particles transitions [16, 17]. In [14] the comparison with the experimental data is performed with use of the leading order (LO) γ^* impact factors (which differ by only trivial coefficients from the analogous ones in QED, which were obtained many years ago [18]), therefore the theoretical predictions have some spread related to the choice of the energy scale s_0. To obtain more definite predictions one needs to know the NLO γ^* impact factors, that makes their evaluation a very important and timely problem.

Knowledge of the NLO Φ_{γ^*} is important not only at energies at which the BFKL dynamics is completely developed, but also in the case when in the BFKL series only a few first terms do contribute (that probably is the case at modern energies). In this case the NLO Φ_{γ^*} determines a size of radiative corrections to the non-decreasing with s contribution to the total cross section.

Recently, the attempts to evaluate Φ_{γ^*} in the NLO have been started [19] - [23]. The impact factors are unambiguosly defined [24] in terms of the effective vertices for the Reggeon-particle interactions. For the evaluation of Φ_{γ^*} one needs to know the amplitude $\Gamma^c_{\gamma^* R \to q\bar{q}}$ for the $q\bar{q}$- pair production in γ^*-Reggeon collision up to the one-loop accuracy as well as the additional gluon emission amplitude $\Gamma^c_{\gamma^* R \to q\bar{q}g}$ at the Born level. They presently are both known [20] -[22] and can be used, in principle, for the NLO Φ_{γ^*} calculation. For this puspose the amplitudes must be squared and integrated over states of the produced particles. But the corresponding expressions are extremely complicated and one can hardly hope to progress with analytical calculations. In this paper we suggest an alternative method to solve this problem based on the use of analytical properties of Feynman diagrams of an effective field theory with the Reggeized gluon. This method allows to consider a part of the diagrams without their real calculation and simplifies considerably the problem. The paper is organized as follows. In the next Section we give a diagrammatic representation for the virtual photon

impact factor. In the Sections 3 and 4 the analytical properties of the Feynman diagrams are discussed and the simplifications due to the analyticity are obtained. The last Section contains our conclusions.

2 Representation of the impact factor

We use the following Sudakov decompositions for the virtual photon and Reggeon momenta p_A and q respectively

$$p_A = p_1 - \frac{Q^2}{s} p_2 \ , \quad p_A^2 = -Q^2 \ , \quad q = \alpha_R p_2 + q_\perp = \frac{\tilde{s} + Q^2 + \vec{q}^{\,2}}{s} p_2 + q_\perp \ , \tag{2.1}$$

$$q^2 = q_\perp^2 = -\vec{q}^{\,2} \ ,$$

where (p_1, p_2) is the light-cone basis of the initial particles momenta plane

$$p_1^2 = p_2^2 = 0 \ , \quad 2p_1 p_2 = s \to \infty \ , \tag{2.2}$$

and $\tilde{s} = (p_A + q)^2$ is the virtual photon - Reggeon squared invariant mass, which is of order of typical transverse momenta, i.e. limited and does not grow with s since the impact factor is related to production of $q\bar{q}$ and $q\bar{q}g$ states in the γ^* fragmentation region. The component of the Reggeon momentum proportional to Sudakov vector p_1 is inessential for the analysis of the impact factor, therefore it is not included in the Eq. (2.1).

The representation of Φ_{γ^*} is quite simple in the LO, where the Reggeized gluon acts as the ordinary gluon with polarization vector p_2/s:

$$\Phi^{(0)}_{\gamma^*}(\vec{q}) \ = \ \frac{1}{\sqrt{N_c^2 - 1}} \sum_{\{a\}} \int \frac{d\tilde{s}}{2\pi} \, |\Gamma^{(0)c}_{\gamma^* R \to q\bar{q}}|^2 \, d\rho_{q\bar{q}} \tag{2.3}$$

where the number of colours $N_c = 3$ for QCD, $\Gamma^{(0)c}_{\gamma^* R \to q\bar{q}}$ is the amplitude of $q\bar{q}$ production in the $\gamma^* R$ collision, evaluated in the Born approximation, $\tilde{s}$ is the squared c.m.s. energy of the $\gamma^* R$ system (equal here the invariant mass of the produced $q\bar{q}$ pair), $d\rho_{q\bar{q}}$ is the phase space element of the pair, see Ref. [25]. The sum $\{a\}$ is over all discrete quantum numbers of the produced pair.

The NLO is not so simple. First of all, Φ_{γ^*} is expressed in terms of $\Gamma^c_{\gamma^* R \to f}$ in more complicated way [24] and depends on the energy scale s_0 in the Mellin transform (1.1):

$$\Phi_{\gamma^*}(\vec{q}, s_0) \ = \ \frac{1}{\sqrt{N_c^2 - 1}} \sum_{\{f\}} \int \frac{d\tilde{s}}{2\pi} \, |\Gamma^c_{\gamma^* R \to f}|^2 \, d\rho_f \, \theta(M^2 - \tilde{s})$$

$$-\frac{g^2 N_c \vec{q}^{\,2}}{(2\pi)^{D-1}} \int \frac{d^{D-2}q_1}{\vec{q}_1^{\,2}(\vec{q}_1-\vec{q})^2} \Phi^{(0)}_{\gamma^*}(\vec{q}_1)\ \ln\frac{M^2}{s_0(\vec{q}_1-\vec{q})^2} - \omega^{(1)}(q^2)\Phi^{(0)}_{\gamma^*}(\vec{q})\ \ln\frac{\vec{q}^{\,2}}{s_0}\,, \tag{2.4}$$

where the sum $\{f\}$ is over all discrete quantum numbers of the contributing states, which are now $q\bar{q}$ and $q\bar{q}g$; $M \to \infty$ is the cut off, which becomes necessary since the integral over $\tilde{s}$ is divergent for the $q\bar{q}g$ state (of course, the dependence on M vanishes due to the cancellation between the first and the second terms); $D = 4 + 2\epsilon$ is the space-time dimension taken different from 4 for regularization of infrared and ultraviolet divergences at intermediate steps. Note that the definition (2.4) provides the infrared finiteness of the impact factor as it was shown explicitly in Ref. [25]. The last two term in (2.4) is the subtraction of the contribution of the gluon emission (real and virtual) outside the fragmentation region of γ^*, which was taken into account already in the LLA;

$$\omega^{(1)}(t) = -\frac{g^2 N_c \Gamma(1-\epsilon)\Gamma^2(\epsilon)}{(4\pi)^{2+\epsilon}\Gamma(2\epsilon)}(\vec{q}^{\,2})^{\epsilon} \tag{2.5}$$

is the gluon Regge trajectory in the one-loop approximation. In the NLO the Reggeon vertices depend on a scale of energy used in the Reggeon factor (see Ref. [26] for details). In the vertices $\Gamma^c_{\gamma^* R\to q\bar{q}}$ entering in (2.4) this scale is taken equal $\vec{q}^{\,2}$.

The second complication is that in the NLO the Reggeon differs essentially from the gluon. Therefore, unlike usual QCD vertices (such as, for example, the quark-quark-gluon vertex) for which we can draw a definite set of Feynman diagrams with perfectly defined rules for calculation of their contributions, we have not such rules for the Reggeon vertices. Usually these vertices are extracted from comparison of appropriate scattering amplitudes with their Reggeized form, so that to obtain a NLO vertex one must calculate radiative corrections to a whole amplitude. Nevertheless, it was shown in Refs. [25], [27], that it is possible to formulate definite rules for calculation the vertices themselves. In the NLO any vertex can be presented as the sum of two contributions, the first of which is equal to $\Gamma^{(0)}\omega^{(1)}\left(q^2\right)(\ln\beta_0 + k/2)$ where $\Gamma^{(0)}$ is the LO vertex, β_0 is an intermediate parameter for separation of two kinematical regions, k is the process independent constant

$$k = \frac{1}{\epsilon} + 2\psi(1+2\epsilon) - 2\psi(1+\epsilon) + \psi(1-\epsilon) - \psi(1) + \frac{5+3\epsilon-2(1+\epsilon)n_f/N_c}{2(1+2\epsilon)(3+2\epsilon)}\,, \tag{2.6}$$

and the second contribution can be obtained as usual one-loop QCD amplitude with ordinary representation in terms of the Feynman diagrams, where for the Reggeized gluon interactions one should use the vertices of Fig. 1.

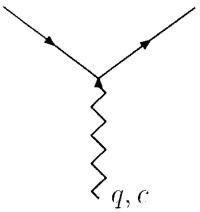

$$= igt^c \frac{\not{p}_2}{s} \ .$$

(a)

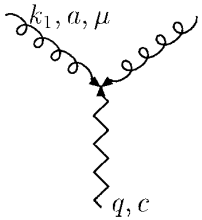

$$= -igT^c_{ab}\left[g^{\mu\nu}\frac{p_2(k_2-k_1)}{s} + \frac{p_2^\mu}{s}(2k_1+k_2)^\nu \right.$$
$$\left. -\frac{p_2^\nu}{s}(2k_2+k_1)^\mu + \frac{2q^2}{s}\frac{p_2^\mu p_2^\nu}{p_2(k_1-k_2)}\right]\theta\left(\left|\frac{p_2(k_1-k_2)}{s}\right| - \beta_0\right) \ .$$

(b)

Figure 1: The quark-quark-Reggeon and the gluon-gluon-Reggeon effective vertices. The zig-zag lines represent the Reggeized gluon; t^c and T^c are the colour group generators in the fundamental and adjoint representations respectively.

Self-energy insertions in the Reggeon line must be omitted and the Feynman gauge for virtual gluons is assumed. In (2.6) $\psi(z) = \Gamma'(z)/\Gamma(z)$, n_f is the number of quark flavours. The intermediate parameter $\beta_0 \to 0$ (remind, however, that first of all the limit $s \to \infty$ must be taken) and dependence on β_0 vanishes in this limit due to the cancellation between the two contributions. The amplitude $\Gamma^c_{\gamma^* R \to q\bar{q}g}$ is needed at the Born level only. It can be calculated using the same Feynman rules (the vertices of Fig. 1 and the Feynman gauge for virtual gluons). Generally speaking, for real emission the theta function in the vertex of Fig. 1 should be absent. But for the real emission the limitation on the invariant mass of the $q\bar{q}g$ system in (2.4) leads to

$$\left|\frac{p_2(k_1-k_2)}{s}\right| \geq \frac{\vec{k}^{\,2}}{M^2} \ , \tag{2.7}$$

where $\vec{k}$ is the transverse momentum of the emitted gluon. We will choose

the parameter $\beta_0 \to 0$ so small that in the region (2.7) the theta function of Fig. 1 is equal 1, so that it can be formally written. The amplitude obtained in such a way is gauge invariant with respect to the emitted gluon, that allows to use the Feynman gauge for summation over its polarizations as well.

Therefore we can present the NLO virtual photon impact factor in the form

$$\Phi_{\gamma^*}(\vec{q}, s_0) = \Phi_M(\vec{q}) - \frac{g^2 N_c \vec{q}^{\,2}}{(2\pi)^{D-1}} \int \frac{d^{D-2}q_1}{\vec{q}_1^{\,2}(\vec{q}_1 - \vec{q})^2} \Phi^{(0)}_{\gamma^*}(\vec{q}_1) \ \ln \frac{M^2}{s_0(\vec{q}_1 - \vec{q})^2}$$

$$+\omega^{(1)}(q^2)\Phi^{(0)}_{\gamma^*}(\vec{q}) \ \left(\ln \frac{s_0 \beta_0^2}{\vec{q}^{\,2}} + k \right) , \qquad (2.8)$$

where k is defined in (2.6) and Φ_M is expressed in terms of the $\tilde{s}$-channel discontinuity of the forward $\gamma^* R$ scattering amplitude:

$$\Phi_M(\vec{q}) = -2i \int_0^{M^2} \frac{d\tilde{s}}{2\pi} \sum_n D_n^{(cut)}(q) = -2i \int_0^{M^2} \frac{d\tilde{s}}{2\pi} \Delta_{\tilde{s}} \sum_l D_l(q) \ . \qquad (2.9)$$

Here D_l is the contribution of l-th diagram to the $\gamma^* R \to \gamma^* R$ amplitude, $\Delta_{\tilde{s}} D_l$ is its $\tilde{s}$-channel discontinuity and $D_n^{(cut)}$ is the contribution to the discontinuity of n-th cut diagram calculated according to Cutcosky rule ($-2\pi i \delta_+(k^2)$ for a cut line with momentum k instead of $1/(k^2 + i0)$ in the amplitude). The factor 2 in (2.9) appears since each diagram has its partner with opposite direction of quark line, which gives the same contribution, and which is not included in the sums in (2.9). There are 34 LO and NLO diagrams for $\gamma^* R$ scattering having the $\tilde{s}$-channel discontinuity, and 56 cut diagrams (some of diagrams have more than one Cutcosky cuts) in the relation (2.9) for the contribution $\Phi_M(\vec{q})$ to the virtual photon impact factor, which we will be mostly concentrated on in the following. We do not present all of them here, but explain our method how to reduce the number of diagrams to be calculated on the example of simple subset of the diagrams shown at the Fig. 2. In spite of the simplicity it contains all the relevant to our discussion features of the complete set of the diagrams of (2.9).

First we notice that the diagrams (a) and (c) of the Fig. 2, as well as the diagrams (b) and (d) there, differ by directions of all external lines only. The replacement $c \leftrightarrow c'$ does not change anything because of the colour singlet in the t- channel. This means that we have to consider, for instance, the first two diagrams of Fig. 2 only, assuming for them

$$e_\mu e'^*_\nu \to e_\mu e'^*_\nu + e'^*_\mu e_\nu \ , \qquad (2.10)$$

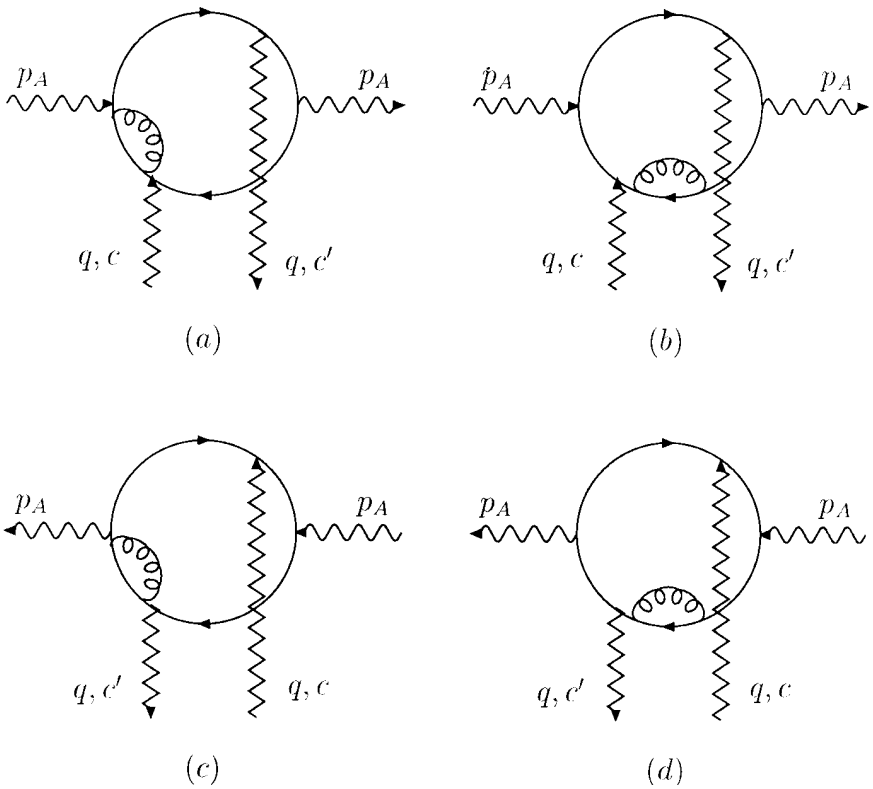

Figure 2: Some of diagrams contributing to Eq. (2.9).

with e and e' being the polarizations of the incoming and outgoing virtual photons correspondingly. Each diagram of the set of Eq. (2.9) either has such partner or is self-symmetric under the symmetrization of the initial and final virtual photons polarizations. Further we always assume the prescription (2.10) for each diagram we work with, that reduces the number of the Feynman diagrams to be considered in the relation (2.9) to 22, 2 (LO) and 20 (NLO) shown in Figs. 4, 5(a) and Fig. 7. In the next Sections we will show how to reduce more this number using the analytical properties of the diagrams.

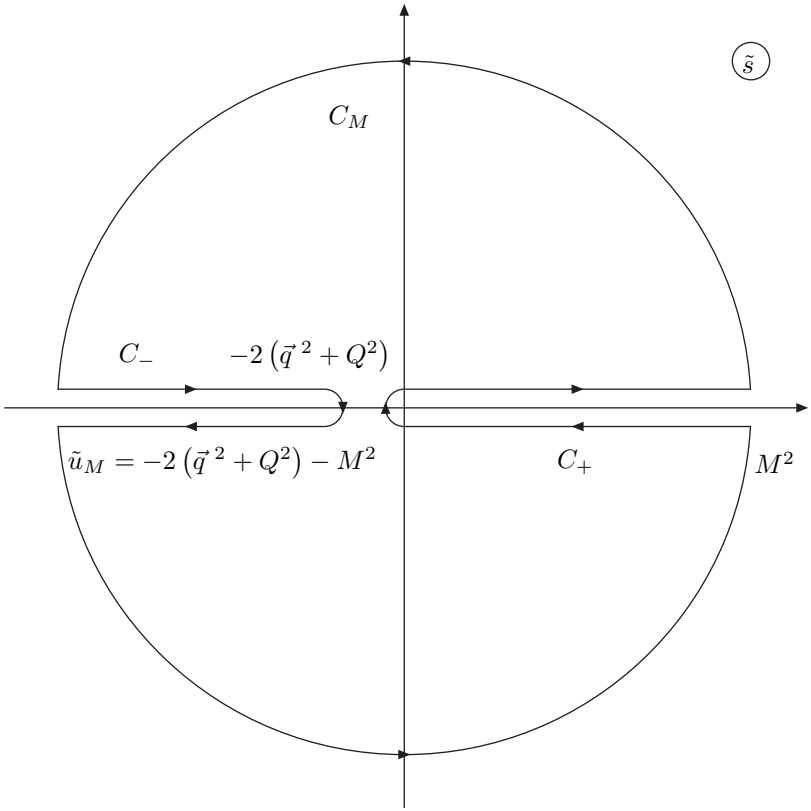

Figure 3: Schematic representation of analytical properties of D_n.

3 Analytical properties of D_n

Let us consider one of the contributions D_n in Eq. (2.9). It is an analytical function $\tilde{s}$ having the cut at $0 < \tilde{s} < \infty$ and, possibly, also the cut at $-\infty < \tilde{s} < -2\left(\vec{q}^{\,2}+Q^2\right)$ related to the $\tilde{u}$- channel Cutcosky cuts with

$$\tilde{u} = (p_A - q)^2 = -2\left(\vec{q}^{\,2}+Q^2\right) - \tilde{s}\ . \tag{3.1}$$

We need the integral (see Fig. 3)

$$\int_0^{M^2} d\tilde{s}\Delta_{\tilde{s}} D_n(q) = \int_{C_+} d\tilde{s} D_n(q) = -\int_{C_M} d\tilde{s} D_n(q) - \int_{C_-} d\tilde{s} D_n(q) \ . \quad (3.2)$$

Using Eqs. (2.1), (3.1), the last integral here can be presented as

$$-\int_{C_-} d\tilde{s} D_n(q) = \int_0^{M^2} d\tilde{u}\Delta_{\tilde{u}} D_n(q) = \int_0^{M^2} d\tilde{s}\Delta_{\tilde{s}} D_n(-q') \quad (3.3)$$

$$= \int_0^{M^2} d\tilde{s}\Delta_{\tilde{s}} \tilde{D}_n(q') \ ,$$

where

$$q' = \frac{\tilde{s} + Q^2 + \vec{q}^{\,2}}{s} p_2 - q_\perp = q\Big|_{q_\perp \leftrightarrow -q_\perp} \ , \quad (3.4)$$

and $\tilde{D}_n$ differs from D_n by the Reggeon line directions only. In the light-cone gauge

$$ep_2 = e'p_2 = 0 \ , \quad (3.5)$$

which we use, contribution of each diagram can be decomposed over four independent spin structures which we define as follows

$$T^{(+)} = \frac{-e_\mu e'^*_\nu}{1+\epsilon} g_\perp^{\mu\nu} \ , \quad T^{(-)} = \frac{-e_\mu e'^*_\nu}{(1+\epsilon)(1+2\epsilon)} \left(g_\perp^{\mu\nu} - (D-2)\frac{q_\perp^\mu q_\perp^\nu}{q_\perp^2} \right) \ ,$$

$$L^{(+)} = e_\mu e'^*_\nu \frac{p_A^\mu p_A^\nu}{Q^2} \ , \quad L^{(-)} = \left(e_\mu e'^*_\nu + e'^*_\mu e_\nu \right) \frac{2p_A^\mu q_\perp^\nu}{\sqrt{2\vec{q}^{\,2} Q^2}} \ , \quad (3.6)$$

where

$$g_\perp^{\mu\nu} = g^{\mu\nu} - \frac{p_1^\mu p_2^\nu + p_2^\mu p_1^\nu}{p_1 p_2} \ . \quad (3.7)$$

The spin structures $T^{(+)}$ and $L^{(+)}$ describe the transverse and the longitudinal spin-non-flip transitions respectively, the other two structures, $T^{(-)}$ and $L^{(-)}$, correspond to the double and the single spin-flip helicity amplitudes. Therefore we come to the conclusion

$$\tilde{D}_n(q') = \tilde{D}_n(q)\Big|_{q_\perp \leftrightarrow -q_\perp} = \tilde{D}_n(q)\Big|_{L^{(-)} \leftrightarrow -L^{(-)}} \ , \quad (3.8)$$

and finally, using Eqs. (3.2), (3.3) and (3.8), we get

$$\int_0^{M^2} d\tilde{s}\Delta_{\tilde{s}} D_n(q) = -\int_{C_M} d\tilde{s} D_n(q) + \int_0^{M^2} d\tilde{s}\Delta_{\tilde{s}}\tilde{D}_n(q)\Big|_{L^{(-)}\leftrightarrow -L^{(-)}} . \quad (3.9)$$

Eq. (3.9) can be written for any diagram in (2.9); for those of them without $\tilde{u}$- channel cut the last term in (3.9) does not appear. Let us consider the application of the relation (3.9) for the diagrams of Fig. 2. According to the discussion above, their contribution to Φ_M takes the form

$$\Phi_M^{(Fig.\ 2)} = -2i\int_0^{M^2} \frac{d\tilde{s}}{2\pi}\Delta_{\tilde{s}}\left(D_{2(a)} + D_{2(b)}\right)$$

$$= 2i\int_{C_M} \frac{d\tilde{s}}{2\pi} D_{2(b)} - 2i\int_0^{M^2} \frac{d\tilde{s}}{2\pi}\Delta_{\tilde{s}}\left(D_{2(a)} + \tilde{D}_{2(b)}\Big|_{L^{(-)}\leftrightarrow -L^{(-)}}\right) , \quad (3.10)$$

where we have applied (3.9) to the diagram $D_{2(b)}$. It is easy to see that

$$\tilde{D}_{2(b)} = D_{2(a)} , \quad (3.11)$$

and therefore

$$\Phi_M^{(Fig.\ 2)} = 2i\int_{C_M} \frac{d\tilde{s}}{2\pi} D_{2(b)} - 4i\int_0^{M^2} \frac{d\tilde{s}}{2\pi}\Delta_{\tilde{s}} D_{2(a)}\Big|_{L^{(-)}=0} . \quad (3.12)$$

It is easy to understand, that each diagram from (2.9) having both $\tilde{s}$- and $\tilde{u}$- channel singularities is either self-symmetric under the replacement $D \leftrightarrow \tilde{D}$ or has the symmetric partner, that is quite natural since the $\tilde{s}$- and $\tilde{u}$-channels are actually the same in the case under consideration. Coming back to our example and comparing Eqs. (3.10) and (3.12), we see, that if we worked in a scalar quantum field theory (let us say ϕ^3 for definiteness) we could consider only one diagram instead of two, because the contribution of the large circle would disappear due to fast enough decrease of amplitudes at large $\tilde{s}$. The situation in QCD is more complicated: contributions from the integration over the large circle basically survive for separate diagrams. Nevertheless, in the following we will show that the analyticity helps to consider many diagrams without their real calculation in the QCD case also.

Using the described analytical properties of D_n one can present the impact factor Φ_M in the form

$$\Phi_M = \Phi_\Delta + \Phi_\Lambda , \quad (3.13)$$

where the first contribution is given by the integral over $\tilde{s}$- channel discontinuity of 12 diagrams of the Fig. 4

$$\Phi_\Delta = -i \int_0^{M^2} \frac{d\tilde{s}}{2\pi} \Delta_{\tilde{s}} \Big[D_{4(a)} + \cdots + D_{4(c)}$$

$$+2 \left(D_{4(d)} + \cdots + D_{4(j)} \right) + 2 \left(D_{4(k)} + 2 D_{4(l)} \right) \Big|_{L^{(-)}=0} \Big] \ . \qquad (3.14)$$

The discontinuity $\Delta_{\tilde{s}}$ in this relation is given by the $\tilde{s}$- channel Cutcosky cuts. There are 18 cut diagrams corresponding to the diagrams of Fig. 4.

The contribution Φ_Λ in Eq. (3.13) consists of the integrals over the large circle from amplitudes related to diagrams of electro-dynamical kind. We consider it in the next Section in much details. As we will see, it is not necessary to calculate really this contribution so that Φ_M can be expressed through Φ_Δ (3.14) only.

4 Large circle contribution

In order to consider the contribution Φ_Λ we introduce the new longitudinal subspace basis (p_1, p_2') with

$$p_2' = \frac{\tilde{s} + Q^2 + \vec{q}^{\,2}}{s} p_2 \ , \quad 2p_1 p_2' = s_1 = \tilde{s} + Q^2 + \vec{q}^{\,2} = \frac{\tilde{s} - \tilde{u}}{2} \ . \qquad (4.1)$$

Therefore

$$q = p_2' + q_\perp \ , \quad p_A = p_1 - \frac{Q^2}{s_1} p_2' \ , \qquad (4.2)$$

and the gauge fixing condition for the external virtual photons remains actually the same (compare with the Eq.(3.5))

$$e p_2' = e' p_2' = 0 \ . \qquad (4.3)$$

Let us first consider the Born contribution to Φ_Λ

$$\Phi_\Lambda^{(0)} = -i \left(e q_f g \right)^2 \frac{\sqrt{N_c^2 - 1}}{4\pi} \int_{C_M} \frac{d\tilde{s}}{s_1^2} D_a^r \ , \qquad (4.4)$$

where eq_f is the quark electric charge and D_a^r is the amplitude corresponding to the diagram of Fig. 5(a), calculated with the following changes with respect to the Feynman rules used before (we adopt these changes everywhere in this Section)

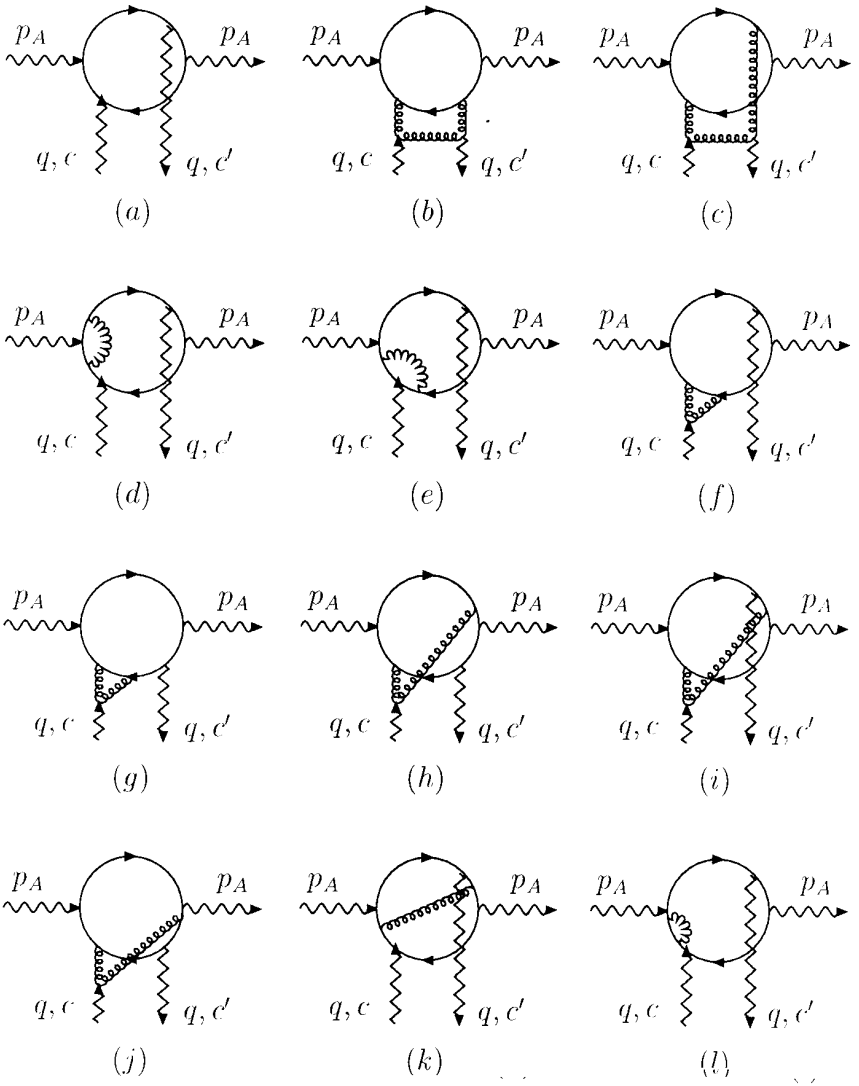

Figure 4: The diagrams contributing to Φ_Δ.

1. $-igt^a$- factors are removed from all QCD vertices as well as $-ieq_f I$ from QED ones so that nothing except corresponding Dirac γ- matrix remains in any vertex;
2. iI from quark propagators and $-i\delta^{ab}$ from gluon ones (they do not appear in D_a^r but they are present in other diagrams for Φ_Λ) are also removed as it is shown in Fig. 5(b);
3. the factor -1 corresponding to the quark loop is omitted;
4. in quark-Reggeon vertices Reggeons are replaced by gluons with polarization vectors equal p_2' (as it is explicitly indicated in the Fig. 5(a)), since the Reggeon interacts with quarks exactly as the gluon with such polarization. Remind that for photon polarizations the substitution (2.10) is assumed.

Using the relation (4.2) together with the above agreement for the Feynman rules, the amplitude D_a^r can be decomposed as it is shown at Fig. 5(c). Then we notice that the last term in Fig. 5(c) with external gluon polarizations $q_\perp$ can be omitted since it does not generate a growing with $\tilde{s}$ contribution required by Eq. (4.4). This is because to obtain the growing contribution at limited transverse polarization vectors of the external gluons one needs purely gluonic intermediate states in the t- channel. So, D_a^r can be presented by the last but one term in the graphic relation of Fig. 5(c). To investigate further its high energy behaviour we apply the Ward identities shown in a graphic form at Fig. 5(d). They allow to present D_a^r in the form given by the first equality of Fig. 6(a).

We then notice that the parts of the diagrams in this equality related to the $q_\perp$- polarizations can be omitted because the corresponding contributions do not grow with $\tilde{s}$. This admits to apply again the Ward identities and obtain the second equality at Fig. 6(a), where the last diagram evidently does not grow with $\tilde{s}$ and can be omitted.

As for the last but one diagram of Fig. 6(a) we note, first of all, that the external virtual photons there have different from p_A momenta (as it is indicated explicitly), so that the corresponding amplitude can grow with $\tilde{s}$. Nevertheless, it can be omitted also. The reason is that the only energy scale for this amplitude is just $\tilde{s}$ and therefore its high energy behaviour in the used by us dimensional regularization is fixed to be $(-\tilde{s})^{\epsilon+1}$, so that its contribution to (4.4) is proportional to the following expression

$$\int_{C_M} \frac{d\tilde{s}}{2\pi i}\,(-\tilde{s})^{\epsilon-1} = -\int_0^{M^2\to\infty} \frac{d\tilde{s}}{2\pi i}\Delta_{\tilde{s}}\,(-\tilde{s})^{\epsilon-1} = -\frac{\sin(\pi\epsilon)}{\pi}\int_0^\infty d\tilde{s}\,(\tilde{s})^{\epsilon-1} = 0\,. \tag{4.5}$$

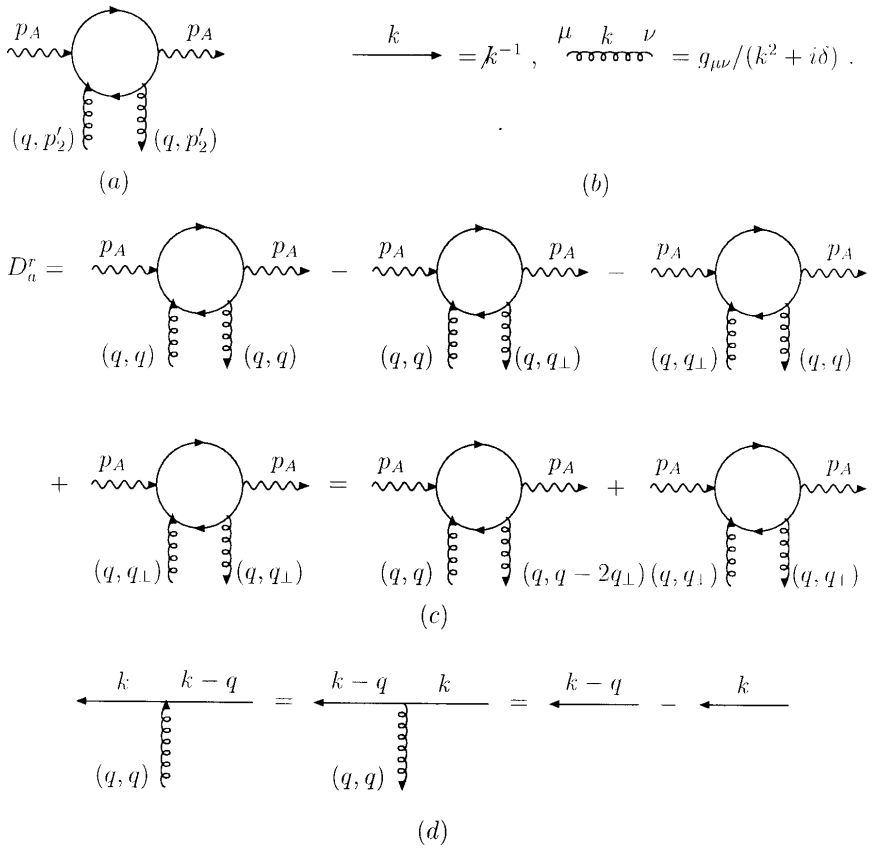

Figure 5: a) the diagram contributing to $\Phi_\Lambda^{(0)}$; b) prescriptions for quark and gluon lines used in Section 4; c) graphic representation of the decompositions of D_a^r; d) the Ward identities in a graphic form.

It vanishes since we first tend M to infinity and only after that ϵ goes to 0, as it is done systematically in the BFKL approach (see Refs. [6] - [10], for instance). Of course, these two limits must commute in final infrared stable results for observables, but at intermediate steps the order of the limits adopted from the beginning must be kept the same everywhere.

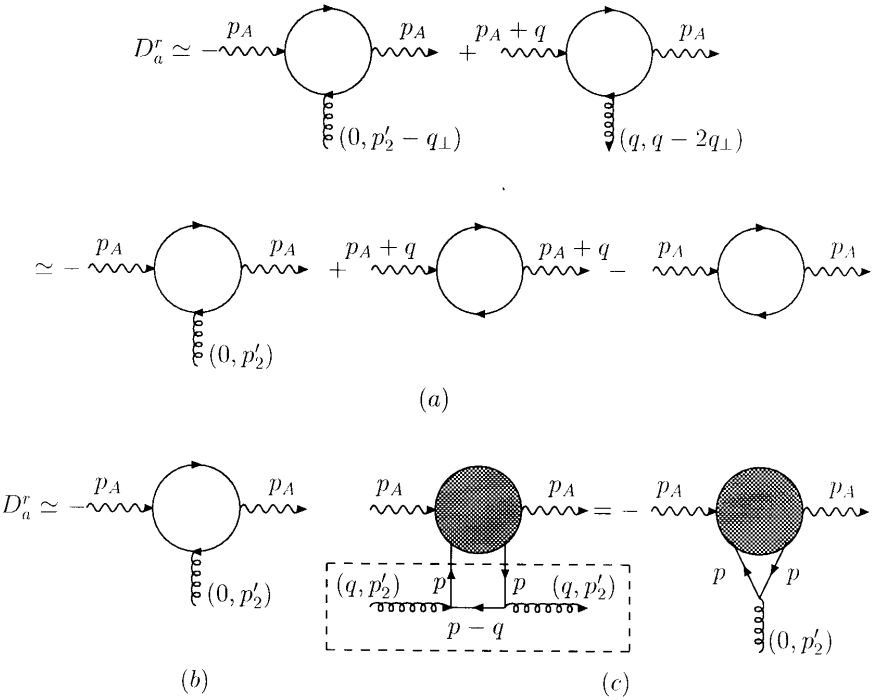

Figure 6: a) decompositions of D_a^r with the use of the Ward identities; b) the final result for the high energy asymptotics of D_a^r; c) the illustration of this final result.

We come therefore to the result for the high energy asymptotics of D_a^r shown graphically in Fig. 6(b). This result demonstrates the complete independence of D_a^r from the Reggeon transverse momentum $q_\perp$. This means the independence from $q_\perp$ also for $\Phi_\Lambda^{(0)}$ itself, and, as we will shortly see, this property is valid for the complete NLO Φ_Λ. Here we make one more remark which will be used in the following: the diagram for D_a^r has a form of the diagram of Fig. 6(c) where the marked by a dash box piece can be written

down as follows

$$\frac{\not p_2'\,(\not p - \not q)\;\not p_2'}{(p-q)^2+i\delta} = -\;\not p_2' + \not p_2' \frac{(\vec p - \vec q)^2 - \alpha\beta s_1}{(1-\alpha)\beta s_1 + (\vec p - \vec q)^2 - i\delta}\;, \tag{4.6}$$

in the Sudakov variables

$$p = \beta p_1 + \alpha p_2' + p_\perp\;. \tag{4.7}$$

At limited transverse momentum

$$\vec p^{\,2} \sim \vec q^{\,2} \sim Q^2\;, \tag{4.8}$$

the essential integration region in the longitudinal subspace is

$$\alpha \sim \vec q^{\,2}/s_1 \ll 1\;, \quad \beta \sim 1\;. \tag{4.9}$$

In this region the last term of Eq. (4.6) is suppressed and can be omitted so that the expression inside the dash box of Fig. 6(c) becomes just

$$\frac{\not p_2'\,(\not p - \not q)\;\not p_2'}{(p-q)^2+i\delta} \to -\;\not p_2'\;. \tag{4.10}$$

As for the region of integration over large transverse momentum, it always brings the energy dependence like that of the Eq. (4.5) and can be also neglected. The prescription (4.10) provides the relation depictured schematically in Fig. 6(c) (of course, it reproduces the correct result for D_a^r).

We now turn to consideration of the complete NLO Φ_Λ which can be written as the sum of three contributions

$$\Phi_\Lambda = \Phi_\Lambda^{(0)} + \Phi_\Lambda^{(1)(a)} + \Phi_\Lambda^{(1)(na)}\;, \tag{4.11}$$

where the LO part $\Phi_\Lambda^{(0)}$ is given by (4.4) and the NLO parts are expressed in terms of 9 diagrams of Fig. 7

$$\Phi_\Lambda^{(1)(a)} = -\left(eq_f g^2\right)^2 \frac{C_F\sqrt{N_c^2-1}}{4\pi}$$

$$\times \int_{C_M} \frac{d\tilde s}{s_1^2}\left[D_1^r + \cdots + D_5^r + 2D_6^r + D_7^r + 2\left(D_8^r + D_9^r\right)\right]\;,$$

$$\Phi_\Lambda^{(1)(na)} = \left(eq_f g^2\right)^2 \frac{C_A\sqrt{N_c^2-1}}{8\pi} \int_{C_M} \frac{d\tilde s}{s_1^2}\left[D_3^r + D_5^r + 2D_8^r\right]\;, \tag{4.12}$$

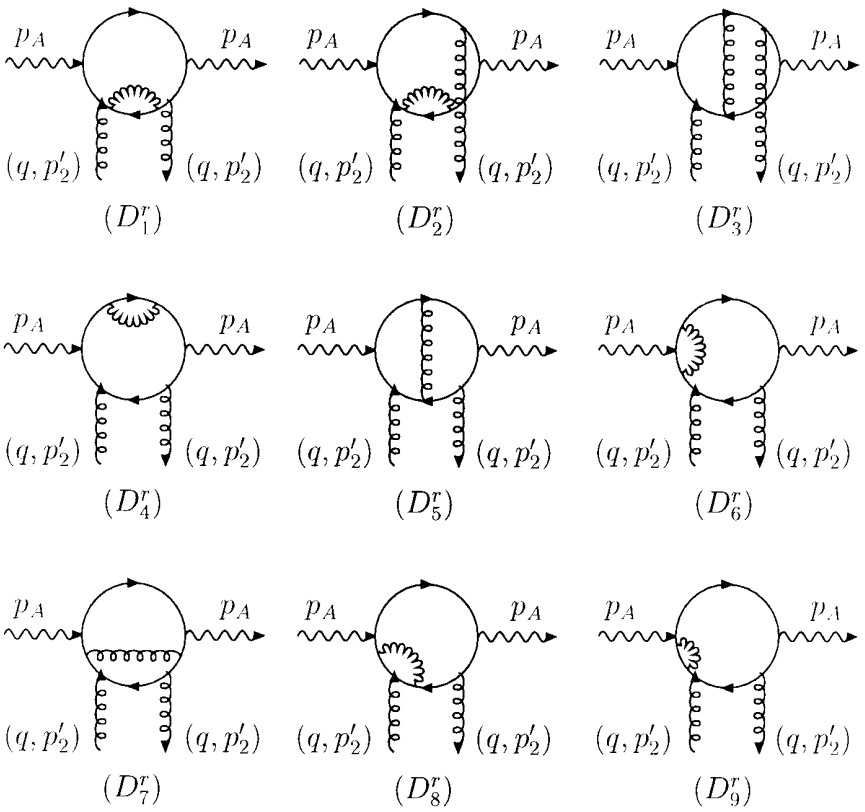

Figure 7: The diagrams contributing to $\Phi_\Lambda^{(1)}$.

with the standard notations C_F and C_A for the Casimir operators in the fundamental and adjoint $SU(N_c)$ colour group representations respectively. For the first three diagrams of Fig. 7 the region of integration over limited transverse momenta does not give a growing with $\tilde{s}$ contribution so that they separately can be omitted due to relations similar to (4.5):

$$\int_{C_M} \frac{d\tilde{s}}{s_1^2} D_1^r = \int_{C_M} \frac{d\tilde{s}}{s_1^2} D_2^r = \int_{C_M} \frac{d\tilde{s}}{s_1^2} D_3^r = 0 \ . \tag{4.13}$$

For other diagrams of Fig. 7, using the Ward identities, one can obtain the relations presented in graphic form by Fig. 8.

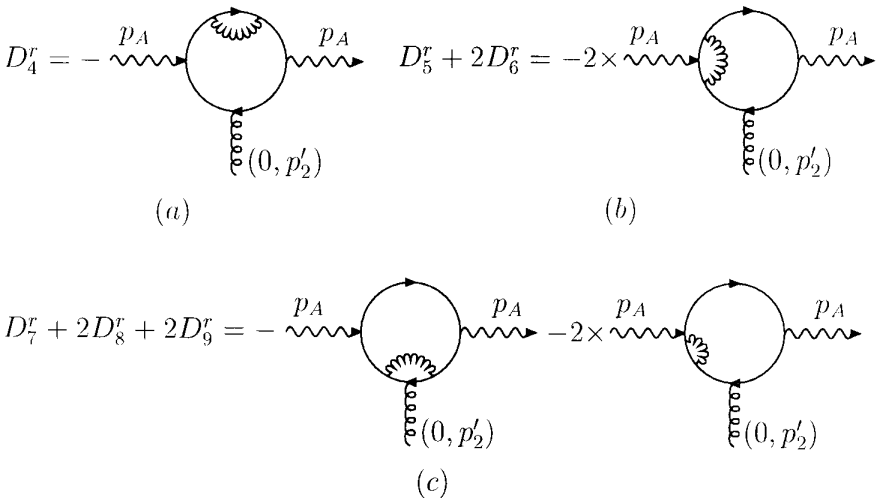

Figure 8: Graphic relations for the diagrams of the Fig. 7.

Let us note that the diagrams for D_4^r, D_6^r, D_7^r and D_9^r are of the kind of Fig. 6(c) and satisfy therefore the same relation in their high energy limit. It means that $2D_6^r$ and $D_7^r + 2D_9^r$ saturate the equalities of Figs. 8(b) and (c) correspondingly, so that D_5^r and D_8^r disappear (separately), although it is not so evident as in the case of the first three diagrams of Fig. 7.

The final conclusion of this Section is that the NLO Φ_Λ consists of the integrals over the large circle in the complex $\tilde{s}$- plane from the amplitudes corresponding to the diagrams presented by Figs. 5(a) and 7, which either have the structure of the Fig. 6(c) and do not therefore depend on $q_\perp$ in the high energy limit or separately disappear in this limit. It leads to the independence from the Reggeon transverse momentum also for the Φ_Λ itself. This conclusion is valid in the Feynman gauge for virtual gluons which we use here.

5 Conclusions

The virtual photon impact factor $\Phi_{\gamma^*}(\vec{q}, s_0)$, being the impact factor of the colourless object, has the property

$$\Phi_{\gamma^*}(\vec{0}, s_0) = 0 \ , \tag{5.1}$$

that is necessary for the infrared finiteness of the cross sections for colourless particles collision. Since the last two terms in (2.8) vanish at $\vec{q}=0$, the contribution $\Phi_M(\vec{q})$ also has this property. We have shown that in the decomposition (3.13) the second term does not depend on $\vec{q}$. It means that $\Phi_M(\vec{q})$ in (2.8) can be presented as

$$\Phi_M(\vec{q}) = \Phi_\Delta(\vec{q}) - \Phi_\Delta(\vec{q}=0) \ , \tag{5.2}$$

where Φ_Δ defined by the Eq. (3.14) and Fig. 4.

We came to the above simplified representation using the analytical properties of the Feynman diagrams of the effective quantum field theory with Reggeized gluon included. A part of the diagrams in the expression (2.9) for the impact factor with known high energy behaviour was moved from the integral over the $\tilde{s}$- channel discontinuity to the integral over the infinite circle in the complex squared energy plane. According to our results this part serves just as a counterterm restoring the correct small $\vec{q}$ behaviour of the other part of the impact factor Φ_Δ, so that it must not be explicitly calculated. In other words, we have performed the cancellation of some irrelevant terms before doing the real calculations. Let us note that the approach using analytical properties of amplitudes of the effective field theory can be useful also for calculation of other NLO impact factors. It is analogous to the approach which was used in QED for the derivation of the sum rules relating the cross sections of various production processes in the Weizsaker-Williams approximation and the slope of the Dirac form factor at zero momentum transfer [28].

To complete our conclusions let us consider how the approach works in the simplest case of the Born virtual photon impact factor. Here we have

$$\Phi^{(0)}_{\gamma^*}(\vec{q}) = \Phi^{(0)}_\Delta(\vec{q}) - \Phi^{(0)}_\Delta(\vec{q}=0) \ , \quad \Phi^{(0)}_\Delta(\vec{q}) = -i\int_0^\infty \frac{d\tilde{s}}{2\pi}\Delta_{\tilde{s}} D_{4(a)} \ , \tag{5.3}$$

where only the first diagram of the Fig. 4 contributes. The calculation becomes very simple and we just quote the result without presentation of any details

$$\Phi^{(0)}_\Delta(\vec{q}) = e^2 g^2 \sqrt{N_c^2-1}\sum_f q_f^2 \frac{\Gamma(1-\epsilon)}{(4\pi)^{2+\epsilon}}\left\{ \left(Q^2\right)^\epsilon \frac{2}{\epsilon}\int_0^1 dx \left(x(1-x)\right)^\epsilon \right.$$

$$\left. \times \left[\left(1+\epsilon\right)\left(1+\epsilon-2x(1-x)\right) T^{(+)} - 4\epsilon x(1-x) L^{(+)} \right] \right.$$

$$+\int_0^1\int_0^1 \frac{dxdy\vec{q}^{\,2}}{\left(y(1-y)\vec{q}^{\,2}+x(1-x)Q^2\right)^{1-\epsilon}}\Big[(1+\epsilon-2x(1-x))$$

$$\times\left(1+\epsilon-2(1+2\epsilon)y(1-y)\right)T^{(+)}+4x(1-x)\left(2(1+2\epsilon)y(1-y)-\epsilon\right)L^{(+)}$$

$$+4(1+2\epsilon)x(1-x)y(1-y)T^{(-)}\Big]\Big\}\,. \tag{5.4}$$

According to our approach the LO virtual photon impact factor itself is given by the above expression without the first term in the curly brackets

$$\Phi^{(0)}_{\gamma^*}(\vec{q})=e^2g^2\sqrt{N_c^2-1}\sum_f q_f^2\frac{\Gamma(1-\epsilon)}{(4\pi)^{2+\epsilon}}\int_0^1\int_0^1\frac{dxdy\vec{q}^{\,2}}{\left(y(1-y)\vec{q}^{\,2}+x(1-x)Q^2\right)^{1-\epsilon}}$$

$$\times\Big[\Big(1+\epsilon-2x(1-x)\Big)\left(1+\epsilon-2(1+2\epsilon)y(1-y)\right)T^{(+)}$$

$$+4x(1-x)\left(2(1+2\epsilon)y(1-y)-\epsilon\right)L^{(+)}+4(1+2\epsilon)x(1-x)y(1-y)T^{(-)}\Big]$$

$$\approx\sqrt{N_c^2-1}\sum_f q_f^2\frac{e^2g^2}{(4\pi)^2}\int_0^1\int_0^1\frac{dxdy\vec{q}^{\,2}}{y(1-y)\vec{q}^{\,2}+x(1-x)Q^2}$$

$$\times\Big[\left(1-2x(1-x)\right)\left(1-2y(1-y)\right)T^{(+)}+8x(1-x)y(1-y)\left(L^{(+)}+\frac{1}{2}T^{(-)}\right)\Big]\,, \tag{5.5}$$

where the last approximate equality shows the result in the physical limit $\epsilon=0$ while the first exact in ϵ equation is necessary in the NLO to evaluate the counterterm in (2.8). Eq. (5.5) restores the well known answer [18] . The calculation in the NLO, instead, remains to be very complicated even with the use of the simplified expression (5.2). Nevertheless, it is to be done since it has a number of the phenomenological applications. We hope to solve this problem in our subsequent publications.

Acknowledgments: Two of us (M.K. and D.I.) thank the Dipartimento di Fisica della Università della Calabria for the warm hospitality while a part of this work was done. D.I. was supported by DFG and BMBF (06OR984). V.S.F. thanks the Alexander von Humboldt foundation for the research award, the Universität Hamburg and DESY for their warm hospitality while a part of this work was done.

References

[1] OPAL Collaboration, G. Abbiendi et al., CERN-EP-2001-06 (2001), hep-ex/0110006.

[2] L3 Collaboration, P. Achard et al., CERN-EP-2001-075 (2001), hep-ex/0111012.

[3] Aleph Collaboration, presented by G. Prange at PHOTONS-2001, Ascona, Switzerland, September 2-7, 2001.

[4] V.S. Fadin, E.A. Kuraev, L.N. Lipatov, Phys. Lett. **B60** (1975) 50;
E.A. Kuraev, L.N. Lipatov and V.S. Fadin, Zh. Eksp. Teor. Fiz. **71** (1976) 840 [Sov. Phys. JETP **44** (1976) 443]; **72** (1977) 377 [**45** (1977) 199];
Ya.Ya. Balitskii and L.N. Lipatov, Sov. J. Nucl. Phys. **28** (1978) 822.

[5] J. Bartels, A. De Roeck, H. Lotter, Phys. Lett. **B389** (1996) 742;
S.J. Brodsky, F. Hautmann, D.E. Soper, Phys. Rev. **D56** (1997) 6957; Phys. Rev. Lett. **78** (1997) 803;
A. Bialas, W. Czyz, W. Florkowski, Eur. Phys. J. **C2** (1998) 683;
M. Boonekamp, A. De Roeck, C. Royon, S. Wallon, Nucl. Phys. **B555** (1999) 540;
J. Kwiecinski, L. Motyka, Acta Phys. Polon. **B30** (1999) 1817; Eur. Phys. J. **C18** (2000) 343.

[6] L.N. Lipatov, V.S. Fadin, Sov. J. Nucl. Phys. **50** (1989) 712.

[7] V.S. Fadin, R. Fiore, M.I. Kotsky, Phys. Lett. **B359** (1995) 181.

[8] V.S. Fadin, R. Fiore, M.I. Kotsky, Phys. Lett. **B387** (1996) 593.

[9] V.S. Fadin, L.N. Lipatov, Nucl. Phys. **B406** (1993) 259.

[10] V.S. Fadin, R. Fiore, A. Quartarolo, Phys. Rev. **D50** (1994) 5893;
V.S. Fadin, R. Fiore, M.I. Kotsky, Phys. Lett. **B389** (1996) 737;
V.S. Fadin, L.N. Lipatov, Nucl. Phys. **B477** (1996) 767;
V.S. Fadin, M.I. Kotsky, L.N. Lipatov, Phys. Lett. **B415** (1997) 97;
V.S. Fadin, R. Fiore, A. Flachi, M.I. Kotsky, Phys. Lett. **B422** (1998) 287.

[11] S. Catani, M. Ciafaloni, F. Hautman, Phys. Lett. **B242** (1990) 97; Nucl. Phys. **B366** (1991) 135;
G. Camici and M. Ciafaloni, Phys. Lett. **B386** (1996) 341; Nucl. Phys. **B496** (1997) 305.

[12] V.S. Fadin, L.N. Lipatov, Phys. Lett. **B429** (1998) 127.

[13] G. Camici and M. Ciafaloni, Phys. Lett. **B430** (1998) 349.

[14] V.T. Kim, L.N. Lipatov, G.B. Pivovariov, Proc. 29th Int. Symposium on Multiparticle Dynamics (ISMD99), Providence, Rhode Island, August 8-13, 1999, hep-ph/9911242; Proc. 8th Blois Workshop (EDS99), Protvino, Russia, June 27 - July 2, 1999, hep-ph/9911228;
S.J. Brodsky, V.S. Fadin, V.T. Kim, L.N. Lipatov, G.B. Pivovariov, presented by V.T. Kim at PHOTONS-2001, Ascona, Switzerland, September 2-7, 2001, hep-ph/0111390.

[15] V.S. Fadin, Proceedings of the 6-th International Workshop on Deep Inelastic Scattering and QCD (DIS98), editors G.H. Coremans and R. Roosen, World Scientific, 1998, p.747-751, hep-ph/9807527.

[16] V.S. Fadin, R. Fiore, M.I. Kotsky and A. Papa, Phys. Rev. **D61** (2000) 094006; Phys. Rev. **D61** (2000) 094005.

[17] M. Ciafaloni, G. Rodrigo, JHEP **0005** (2000) 042, hep-ph/0004033.

[18] H. Cheng, T.T. Wu, Phys. Rev. **D1** (1970) 2775;
G.V. Frolov, V.N. Gribov, L.N. Lipatov, Phys. Lett. **31B** (1970) 34;
V.N. Gribov, L.N. Lipatov, G.V. Frolov, Yad. Fiz. **12** (1971) 994 [Sov. J. Nucl. Phys. **12** (1971) 543].

[19] V. Fadin, D. Ivanov, M. Kotsky, "New Trends in High-Energy Physics", ed. L.L. Jenkovszky, Kiev, 2000, p.190-194, hep-ph/0007119.

[20] J. Bartels, S. Gieseke, C.F. Qiao, Phys. Rev. **D63** (2001) 056014, hep-ph/0009102.

[21] V. Fadin, D. Ivanov, M. Kotsky, Phys. Atom. Nucl. **65**(8) (2002) 1513; hep-ph/0106099.

[22] J. Bartels, S. Gieseke, A. Kyrieleis, Phys. Rev. **D65** (2002) 014006, hep-ph/0107152.

[23] J. Bartels, D. Colferai, S. Gieseke, A. Kyrieleis, hep-ph/0208130.

[24] V.S. Fadin, R. Fiore, Phys. Lett. **B440** (1998) 359.

[25] V.S. Fadin, A.D. Martin, Phys. Rev. **D60** (1999) 114008.

[26] V.S. Fadin, preprint BudkerINP 98-55, hep-ph/9807528, talk given at the International conference "LISHEP98", February 14-20, 1998, Rio de Janeiro, Brazil.

[27] V.S. Fadin, R. Fiore, Phys. Rev. **D64** (2001) 114012, hep-ph/0107010.

[28] E. Kuraev, L. Lipatov, N. Merenkov, Phys. Lett. **B47** (1973) 33.

V.S. Fadin, D.Yu. Ivanov and M.I. Kotsky

On the calculation of the NLO virtual photon impact factor

В.С. Фадин, Д.Ю. Иванов, М.И. Коцкий

О вычислении импакт фактора виртуального фотона

Budker INP 2002-60

Ответственный за выпуск А.М. Кудрявцев
Работа поступила 23.09.2002 г.

Сдано в набор 30.09.2002 г.
Подписано в печать 1.10.2002 г.
Формат бумаги 60×90 1/16 Объем 1.3 печ.л., 1.0 уч.-изд.л.
Тираж 95 экз. Бесплатно. Заказ № 60

Обработано на IBM PC и отпечатано на
ротапринте ИЯФ им. Г.И. Будкера СО РАН
Новосибирск, 630090, пр. академика Лаврентьева, 11.